Cellular and Molecular Neurobiology (2019) 39:823–831
https://doi.org/10.1007/s10571-019-00682-8

ORIGINAL RESEARCH

# Cathepsin K Knockout Exacerbates Haemorrhagic Transformation Induced by Recombinant Tissue Plasminogen Activator After Focal Cerebral Ischaemia in Mice

**Rong Zhao[1] · Xin-Wei He[1] · Yan-Hui Shi[1] · Yi-Sheng Liu[1] · Feng-Di Liu[1] · Yue Hu[1] · Mei-Ting Zhuang[1] · Xiao-Yan Feng[1] · Lei Zhao[1] · Bing-Qiao Zhao[2] · Hui-Qin Liu[3] · Guo-Ping Shi[4] · Jian-Ren Liu[1]**

Received: 22 December 2018 / Accepted: 29 April 2019 / Published online: 7 May 2019


## Abstract

Severe haemorrhagic transformation (HT), a common complication of recombinant tissue plasminogen activator (rtPA) treatment, predicts poor clinical outcomes in acute ischaemic stroke. The search for agents to mitigate this effect includes investigating biomolecules involved in neovascularization. This study examines the role of Cathepsin K (Ctsk) in rtPA-induced HT after focal cerebral ischaemia in mice. After knockout of Ctsk, the gene encoding Ctsk, the outcomes of $Ctsk^{+/+}$ and $Ctsk^{-/-}$ mice were compared 24 h after rtPA-treated cerebral ischaemia with respect to HT severity, neurological deficits, brain oedema, infarct volume, number of apoptotic neurons and activated microglia/macrophage, blood–brain barrier integrity, vascular endothelial growth factor (VEGF) expression and Akt-mTOR pathway activation. We observed that haemoglobin levels, brain oedema and infarct volume were significantly greater and resulted in more severe neurological deficits in $Ctsk^{-/-}$ than in $Ctsk^{+/+}$ mice. Consistent with our hypothesis, the number of NeuN-positive neurons was lower and the number of TUNEL-positive apoptotic neurons and activated microglia/macrophage was higher in $Ctsk^{-/-}$ than in $Ctsk^{+/+}$ mice. Ctsk knockout mice exhibited more severe blood–brain barrier (BBB) disruption, with microvascular endothelial cells exhibiting greater VEGF expression and lower ratios of phospo-Akt/Akt and phospo-mTOR/mTOR than in $Ctsk^{+/+}$ mice. This study is the first to provide molecular insights into Ctsk-regulated HT after cerebral ischaemia, suggesting that Ctsk deficiency may disrupt the BBB via Akt/mTOR/VEGF signalling, resulting in neurological deficits and neuron apoptosis. Ctsk administration has the potential as a novel modality for improving the safety of rtPA treatment following stroke.

**Keywords** Cathepsin K · Haemorrhagic transformation · Ischaemic stroke · Akt · mTOR · VEGF

Rong Zhao, Xin-Wei He, Yan-Hui Shi and Yi-Sheng Liu contributed equally to this work and should be considered co-first authors.

✉ Guo-Ping Shi
gshi@bwh.harvard.edu

✉ Jian-Ren Liu
liujr021@sjtu.edu.cn

[1] Department of Neurology, Shanghai Ninth People's Hospital, Shanghai Jiao Tong University School of Medicine, 639 Zhizaoju Road, Huangpu District, Shanghai 200011, People's Republic of China

[2] State Key Laboratory of Medical Neurobiology, Institutes of Brain Science, Collaborative Innovation Center for Brain Science and School of Basic Medical Sciences, Fudan University, Shanghai, People's Republic of China

[3] Department of Neurology, Henan Provincial People's Hospital, Henan University, Zhengzhou, People's Republic of China

[4] Cardiovascular Medicine, Department of Medicine, Brigham and Women's Hospital and Harvard Medical School, NRB-7, 77 Avenue Louis Pasteur, Boston, MA 02115, USA

## Introduction

Stroke is a leading cause of morbidity and mortality in developed countries, with an immense number of medical care resources devoted to combatting its debilitating consequences. Reperfusion with the thrombolytic agent recombinant tissue plasminogen activator (rtPA) remains the standard treatment for acute ischaemic stroke (AIS) (Morris 2008; Wardlaw et al. 2013). However, the use of rtPA is severely limited by its association with haemorrhagic transformation (HT), the most significant cause of morbidity and mortality in AIS patients (Lansberg et al. 2007; Pena et al. 2017). Indeed, less than 5% of all AIS patients are eligible for rtPA treatment (Khurana et al. 2017). The development of a new strategy for attenuating the severity of HT would significantly increase the overall efficacy of rtPA thrombolytic therapy, ultimately improving the outcomes of AIS patients.

HT is caused by the breakdown of the blood–brain barrier (BBB) after vessel reperfusion following stroke (Sumii and Lo 2002). Further rupture of the BBB damages the entire neurovascular unit, including the extracellular matrix, endothelial cells, astrocytes, neurons and pericytes (Wang and Lo 2003). While BBB breakdown can occur in the absence of intervention (Hong et al. 2014; Jickling et al. 2014; Nour et al. 2013), treatment with rtPA can aggravate BBB disruption and increase the risk of HT (Wang et al. 2015). While the precise mechanism whereby rtPA induces HT is still unclear, studies implicate multiple factors, including tissue-remodelling proteases (Khurana et al. 2017). Among these proteases are cathepsins, a family of lysosomal enzymes involved in vascular remodelling, angiogenesis and atherosclerosis (Bohley and Seglen 1992). In response to disturbed blood flow, cathepsins are activated to remodel the extracellular matrix and modify arterial walls (Platt and Shockey 2016). Hypoxia also has been observed to induce the activation of cathepsins that degrade the vascular matrix (Fukuda et al. 2004). Thus, the involvement of cathepsins in reperfusion injury and HT after stroke is of interest.

Cathepsin K (Ctsk), an essential enzyme in extracellular matrix metabolism, possesses both type I collagenase and elastase activity (Novinec et al. 2007). Highly expressed in osteoclasts, Ctsk is implicated in the pathogenesis of osteoporosis and other bone diseases. In addition, the expression of Ctsk, the gene encoding Ctsk, is upregulated in several vascular diseases, including arteriosclerosis and aortic abdominal aneurysms. An imbalance between Ctsk and its inhibitor is suspected of promoting cerebral aneurysm rupture via excessive breakdown of the extracellular matrix in arterial walls (Aoki et al. 2008). Ctsk is expressed in the human brain (Bernstein et al. 2007), and Ctsk activity is important in the development and maintenance of the CNS in mice (Dauth et al. 2011, 2012). In response to hypoxia, Ctsk was observed to activate Notch1, a protein critical to angiogenesis, resulting in neovascularisation after femoral artery ligation-induced ischaemia in mice (Jiang et al. 2014). Together, these observations warrant investigation of the involvement of Ctsk in vessel remodelling after stroke.

This study investigates whether Ctsk plays a role in rtPA-induced HT. We compare Ctsk knockout and wild-type mice after rtPA treatment of experimentally induced cerebral ischaemia with respect to the severity of HT, neurological deficits, brain oedema and infarct volume, neuron and IBA-1-positive cell expression, BBB integrity and permeability and Akt/mTOR/VEGF signalling pathway activity.

## Materials and Methods

### Animals

Ctsk knockout ($Ctsk^{-/-}$) mice were generated and bred as previously described (Saftig et al. 1998). Ctsk knockout mice survive and are fertile; they manifest no overt phenotypic abnormalities until the age of 10 months (Saftig et al. 1998). The suppressed growth seen in pycnodysostosis patients was not observed in cathepsin K-deficient mice (Saftig et al. 1998). A total of 32 $Ctsk^{-/-}$ and 32 wild-type ($Ctsk^{+/+}$) adult male mice (8–10 weeks old) were used in the cerebral ischaemia and rtPA-induced HT mouse model. In addition, 32 wild-type adult male mice (8–10 weeks old) were used as the sham-surgery group. The experiments were done in a blinded manner. Mice were selected by one experimenter and no other experimenters were informed about the species and grouping of mice; another experimenter made the animal model and another two experimenters performed post-operative evaluation and sample collection and analysis. All mice were maintained at the Animal Center of Shanghai Ninth People's Hospital according to the Guidelines for the Care and Use of Laboratory Animals (National Institutes of Health). All experiments related to the animal studies were approved by the Institutional Animal Care and Use Committee (IACUC) at Shanghai Ninth People's Hospital Animal Center (No. HKDL2017411).

### Cerebral Ischaemia and rtPA-Induced HT Mouse Model

Cerebral ischaemia was induced as described previously (Shahjouei et al. 2016). In brief, transient right middle cerebral artery occlusion (MCAO) was induced by placing a 7.0-siliconised filament through the external carotid artery. After 60 min, the filament was removed to allow reperfusion.

Mice were anesthetised with 1.5% isoflurane in 30% oxygen. Body temperature was maintained at 37 ± 0.5 °C using a heating pad. Laser Doppler Flowmetry was used in all mice to confirm the induction of ischaemia and reperfusion. To increase the extent of cerebral haemorrhage, D-glucose (6 mL/kg at 50% wt/vol) was injected intraperitoneally 15 min before MCAO. Glucose was used because animal and human studies have shown that hyperglycaemia increases the risk of rtPA-induced cerebral haemorrhage after ischaemic stroke (Wang et al. 2013). After 50 min of MCAO, rtPA (10 mg/kg) was administered as an intravenous bolus injection via femoral vein (1 mg/kg) followed by a 9-mg/kg infusion administered with a syringe infusion pump (World precision Instruments) for 30 min.

To examine the influence of Ctsk on rtPA-induced HT after cerebral ischaemia, MCAO and HT were induced in wild-type ($Ctsk^{+/+}$/MCAO/rtPA) and $Ctsk^{-/-}$ ($Ctsk^{-/-}$/MCAO/rtPA) mice. The sham-surgery group was subjected to the same surgical procedure but without the filament thread insertion.

### Quantification of Cerebral Haemorrhage

At 24 h after MCAO, the mice in all three groups ($n = 8$ each) were killed by overdose of chloral hydrate and perfused transcardially with ice-cold PBS. The haemoglobin content was determined to assess the severity of haemorrhage. Drabkin reagent (500 µL) was added to the ischaemic brain tissue of each mouse, followed by homogenisation and centrifugation at 13,000 rpm for 30 min. The supernatant optical density was measured by spectrophotometry (Thermo BioMate 3S; Thermo Scientific) at 540 nm (Wang et al. 2013).

### Neurologic Deficit Score

At 24 h after MCAO, the three groups of mice ($n = 12$ each) were examined and scored blindly for neurologic deficits as follows: 0—no neurological deficit; 1—failure to fully extend left forepaw; 2—reduced resistance to lateral push; 3—spontaneous circling to left; 4—absence of spontaneous movement or unconsciousness (Wang et al. 2013).

### Brain Infarct Volume and Oedema Volume

The infarct volume was determined 24 h after MCAO. The brains of the mice in all three groups ($n = 6$ each) were quickly removed, sectioned coronally at 2-mm intervals and stained by immersion in the vital dye 2% 2,3,5-triphenyltetrazolium hydrochloride at 37 °C for 30 min. The extents of the normal and infarcted areas were analysed using ImageJ (National Institutes of Health, Bethesda, MD, USA) and determined indirectly as follows: Infarct volume = (contralateral hemisphere volume − non-ischaemic ipsilateral hemisphere volume)/contralateral hemisphere volume × 100; Oedema volume = (ipsilateral hemisphere volume − contralateral hemisphere volume)/contralateral hemisphere volume × 100.

### Evaluation of BBB Permeability

At 24 h after MCAO, the mice in all three groups ($n = 6$ each) were injected intravenously with 2% Evans blue dye (2 mL/kg body weight) and allowed to circulate for 60 min. Animals were perfused transcardially with PBS, and their brains were removed and placed in formamide for 72 h. The amount of extravasated dye was evaluated by spectrophotometry (Thermo BioMate 3S; Thermo Scientific, Waltham, MA) at 620 nm.

### Western Blot Analysis

Ischaemic hemispheric brain tissues and matching tissues from sham-surgery mice ($n = 6$) were dissected. The brain tissues were homogenised in RIPA lysis buffer including a protease inhibitor cocktail (Roche Diagnostics, Mannheim, Germany). After centrifugation, the protein concentration was determined by BCA protein assay. Equal amounts of protein were loaded onto a 10% Tris–glycine gel, electrophoresed and transferred onto polyvinylidene difluoride membranes. Membranes were blocked with 5% non-fat dry milk in Tris-buffered saline with 0.1% Tween-20 and probed with primary antibodies, followed by incubation at 4 °C overnight with primary antibodies at the following dilution: NeuN(rabbit monoclonal antibody, MAB377, Millipore, Massachusetts, USA),1:1000; Occludin (rabbit monoclonal antibody, ab167161, Abcam, Cambridge, UK), 1:1000; Claudin-5 (rabbit monoclonal antibody, 35-2500, Thermo Fisher Scientific), 1:1000; VEGF (rabbit monoclonal antibody, ab1316, Abcam), 1:1000; Akt (rabbit polyclonal antibody, ab8805, Abcam), 1:1000; p-Akt (rabbit polyclonal antibody, ab66138, Abcam), 1:1000; mTOR (rabbit polyclonal antibody, ab2732, Abcam), 1:1000; p-mTOR (rabbit monoclonal antibody, ab109268, Abcam), 1:1000 and beta-actin (rabbit monoclonal antibody, #4970, Cell Signaling Technology, Beverly, MA), 1:1000. For each primary antibody, the appropriate horseradish peroxidase-conjugated secondary antibody was used. The target bands were visualised using enhanced chemiluminescence reagent and quantified by scanning densitometry using Bio-Image Analysis System. The intensity of target protein bands was standardised to the intensity of β-actin bands.

### Immunofluorescence Staining

Twenty-four hours after MCAO, the three groups of mice ($n=6$ each) were killed by overdose of chloral hydrate and perfused transcardially with ice-cold PBS and 4% paraformaldehyde. The brains were removed and cryoprotected in 30% sucrose in PBS. Brain cryosections (20 μm) were blocked with 1% bovine serum albumin and 5% normal donkey serum in PBS and incubated with anti-NeuN (rabbit monoclonal antibody, MAB377, Millipore, Massachusetts, USA) or anti-IBA-1 (rabbit monoclonal antibody, ab178847, Abcam) or a combination of anti-VEGF (rabbit monoclonal antibody, ab1316, Abcam) and anti-CD31 antibodies (rat monoclonal antibody, PECAM-1, BD Pharmingen) overnight at 4 °C. The sections were then rinsed and incubated with Alexa Fluor 594 goat anti-rabbit IgG (#8889, Cell Signaling Technology) or Alexa Fluor 488 goat anti-rabbit IgG (#4412, Cell Signaling Technology), or a mixture of Alexa Fluor 594 goat anti-rabbit IgG and Alexa Fluor 488 donkey anti-rat IgG (A21208, Invitrogen) for 1 h at room temperature. Images were obtained using a Leica microscope. For the quantification of NeuN-positive cells and IBA-1-positive cells and the area of double-positive CD31 and VEGF cells, 5 non-overlapping images in the peri-infarct area were digitised using a ×40 objective, two of them were located in the cortex and three in the basal ganglia. The images were selected by a researcher who did not know the grouping information. The images were processed by NIH ImageJ and contrast enhanced to clearly differentiate positivity from background. For each brain, three sections from the ischaemic hemisphere were analysed.

### TUNEL Assay

Apoptotic cells were identified by TUNEL assay (11684817910, Roche Diagnostics, Mannheim, Germany), and the total cell number was counted after DAPI (4′,6-diamidino-2-phenylindole) staining. Coronal cryosections from at least five mice in each group were obtained. Five random fields in the peri-infarct area of each section were digitised using a ×40 objective. The results are expressed as the percentage of $TUNEL^+/DAPI^+$ cells in the section.

### Statistical Analysis

All continuous variables are presented in bar graphs (mean ± SEM). For each figure, the error bars indicated SEM. Differences were assessed using Student's *t* test for 2-group comparisons. Ranked data (neurological deficit scores) are presented as median (interquartile range, IQR) and in box-plot figures, and non-parameter Mann–Whitney U test is used for 2-group comparisons. Two-tailed $p<0.05$ was considered statistically significant. All graphing and analyses were performed using SAS 9.4 software (SAS Institute Inc., Cary, NC, USA.).

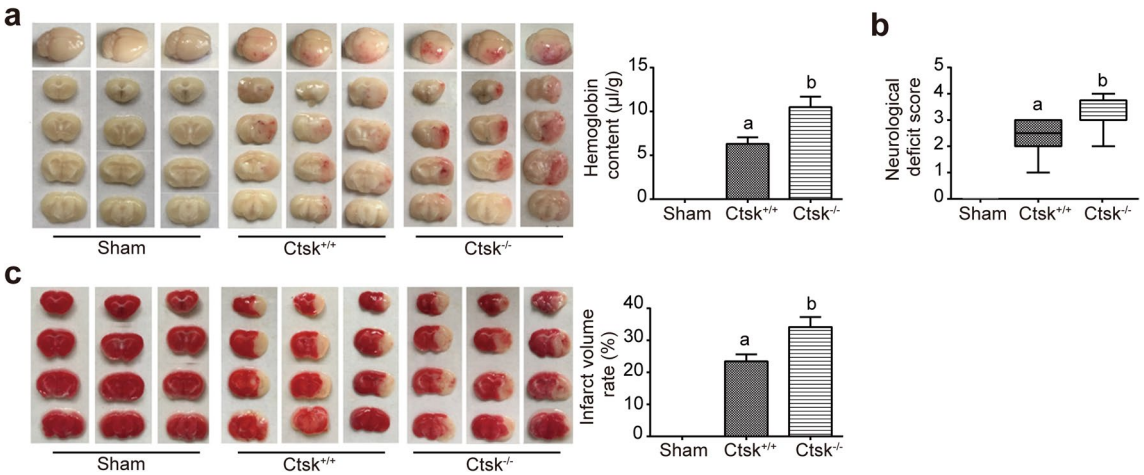


**Fig. 1** Greater degree of HT and worse outcomes in $Ctsk^{-/-}$/MCAO/rtPA mice. **a** *Left panel*, images of whole brain sections of mice from each group. *Right panel*, haemoglobin content was greater in $Ctsk^{-/-}$/MCAO/rtPA ($Ctsk^{-/-}$) mice than in $Ctsk^{+/+}$/MCAO/rtPA ($Ctsk^{+/+}$) mice. **b** $Ctsk^{-/-}$/MCAO/rtPA mice showed more severe neurologic deficits than $Ctsk^{+/+}$/MCAO/rtPA mice. **c** *Left panel* TTC staining of HT in brain sections from mice of each group. *Right panel* larger infarct volume observed in $Ctsk^{-/-}$/MCAO/rtPA than in $Ctsk^{+/+}$/MCAO/rtPA mice. $^a p<0.05$, sham versus $Ctsk^{+/+}$; $^b p<0.05$, $Ctsk^{-/-}$ versus $Ctsk^{+/+}$

## Results

### Ctsk Deficiency Increased the Neurological Deficits and Infarct Volume in MCAO/rtPA-Induced HT Mice

To examine the influence of Ctsk expression on rtPA-induced HT after cerebral ischaemia, the degree of HT after cerebral ischaemia (Fig. 1a) was compared between $Ctsk^{+/+}$ and $Ctsk^{-/-}$ mice. Spectrophotometric haemoglobin assay showed that haemoglobin concentrations were significantly higher in $Ctsk^{-/-}$/MCAO/rtPA mice than in $Ctsk^{+/+}$/MCAO/rtPA mice (Fig. 1a) at 24 h after stroke. $Ctsk^{-/-}$/MCAO/rtPA mice showed more severe neurological deficits as assessed by neurological scores than did $Ctsk^{+/+}$/MCAO/rtPA mice (Fig. 1b). Analysis of TTC-stained brain sections showed that the infarct volume was significantly larger in $Ctsk^{-/-}$/MCAO/rtPA mice than in $Ctsk^{+/+}$/MCAO/rtPA mice (Fig. 1c).

### Ctsk Knockout Increased the Number of Apoptotic Neurons and Activated Microglia/Macrophage in MCAO/rtPA-Induced HT Mice

To study the role of Ctsk in neuron expression and microglia/macrophage activation, the expression of NeuN and IBA-1 in the peri-infarct area was determined. $Ctsk^{+/+}$/MCAO/rtPA mice had significantly fewer NeuN-positive cells and lower NeuN protein expression levels than did sham-surgery mice (Fig. 2a, b). However, $Ctsk^{+/+}$/MCAO/rtPA mice had more NeuN-positive cells and greater NeuN protein expression than did $Ctsk^{-/-}$/MCAO/rtPA mice (Fig. 2a, b). The number of TUNEL-positive cells was significantly greater in $Ctsk^{+/+}$/MCAO/rtPA mice than in sham-surgery mice, with more TUNEL-positive cells in $Ctsk^{-/-}$/MCAO/rtPA mice than in $Ctsk^{+/+}$/MCAO/rtPA mice (Fig. 2c). Immunostaining revealed that the number of IBA-1-positive cells (microglia cells/macrophages) was significantly higher in $Ctsk^{+/+}$/MCAO/rtPA mice than in sham-surgery mice, with significantly more IBA-1-positive cells in $Ctsk^{-/-}$/MCAO/rtPA than in $Ctsk^{+/+}$/MCAO/rtPA mice (Fig. 2d).

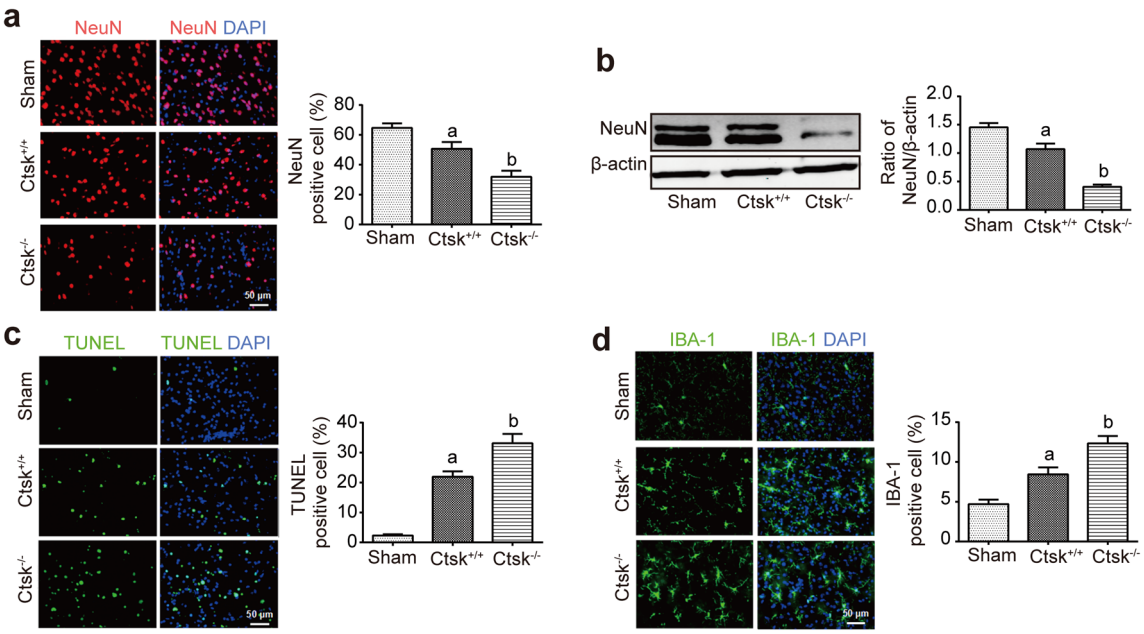


**Fig. 2** Neuron damage and IBA-1 positive cell activation elevated in $Ctsk^{-/-}$/MCAO/rtPA mice. **a** Comparison of brain coronal sections immunostained with anti-NeuN (red) and DAPI (blue). Neurons were identified as $NeuN^+$ and $DAPI^+$cells in brain sections. The number of neurons was lower in $Ctsk^{+/+}$/MCAO/rtPA ($Ctsk^{+/+}$) mice compared with the sham-surgery group and lower in $Ctsk^{-/-}$/MCAO/rtPA than $Ctsk^{+/+}$/MCAO/rtPA mice. **b** Western blot of NeuN and β-actin loading control in ischaemic hemispheres lysates from mice of different groups. Quantification of NeuN from western blots shows lower expression in $Ctsk^{+/+}$/MCAO/rtPA mice than in sham mice, with lower expression in $Ctsk^{-/-}$/MCAO/rtPA than $Ctsk^{+/+}$/MCAO/rtPA mice. **c** The number of apoptotic cells was determined by counting TUNEL + (green) and DAPI + (blue) cells. The number of apoptotic cells was higher in $Ctsk^{+/+}$/MCAO/rtPA mice than in sham-surgery mice, with more apoptotic cells in $Ctsk^{-/-}$/MCAO/rtPA than in $Ctsk^{+/+}$/MCAO/rtPA mice. **d** Comparison of brain coronal sections immunofluorescently stained with anti-IBA (green) and DAPI (blue) between mice of different groups. Activated microglia or microphage were identified as $IBA^+/DAPI^+$ cells in brain sections. The number of activated microglia or microphage was greater in $Ctsk^{+/+}$/MCAO/rtPA mice than in sham-surgery mice, with more activated microglia or microphage in $Ctsk^{-/-}$/MCAO/rtPA than in $Ctsk^{+/+}$/MCAO/rtPA mice. $^a p < 0.05$, sham versus $Ctsk^{+/+}$; $^b p < 0.05$, $Ctsk^{-/-}$ versus $Ctsk^{+/+}$

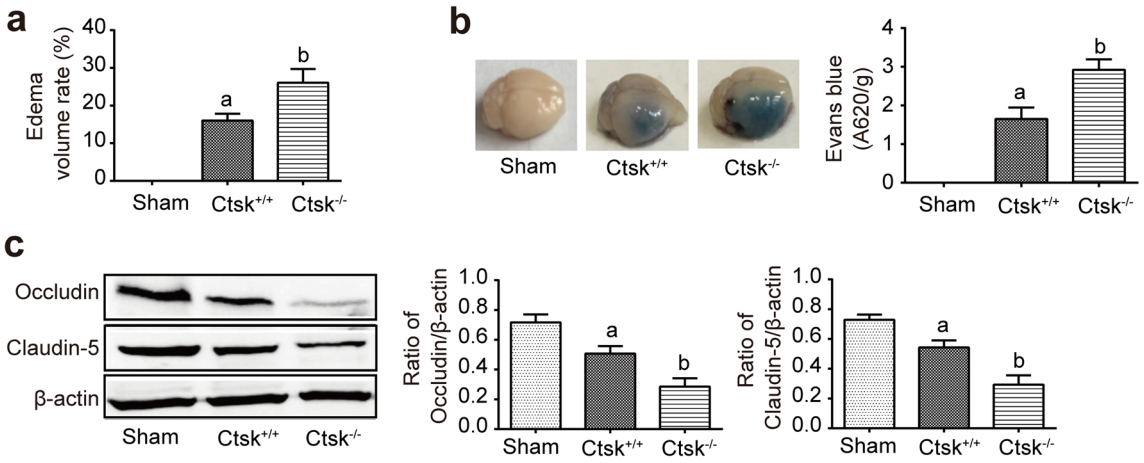


**Fig. 3** Greater BBB disruption in Ctsk$^{-/-}$/MCAO/rtPA mice. **a** The oedema volume was greater in Ctsk$^{-/-}$/MCAO/rtPA (Ctsk$^{-/-}$) than in Ctsk$^{+/+}$/MCAO/rtPA (Ctsk$^{+/+}$) mice, as evidenced by TTC staining. **b** *Left panel* images of whole brains from mice of different groups after EB treatment. *Right panel* significantly more extravasated EB dye was seen in Ctsk$^{-/-}$/MCAO/rtPA than in Ctsk$^{+/+}$/MCAO/rtPA mice. **c** Expression of occludin, claudin-5 and β-actin loading control in the ischaemic hemisphere lysates from mice of different groups were analysed by western blot. Occludin and claudin-5 expression was higher in Ctsk$^{-/-}$/MCAO/rtPA than in Ctsk$^{+/+}$/MCAO/rtPA mice. $^{a}p < 0.05$, sham versus Ctsk$^{+/+}$; $^{b}p < 0.05$, Ctsk$^{-/-}$ versus Ctsk$^{+/+}$

## Ctsk Knockout Disrupts BBB Integrity and Permeability in MCAO/rtPA-Induced HT Mice

The oedema volume was greater in Ctsk$^{-/-}$/MCAO/rtPA than in Ctsk$^{+/+}$/MCAO/rtPA mice (Fig. 3a). Studies of BBB function, as evaluated using the Evans blue assay 24 h after MCAO, showed marked extravasation of EB dye in the ischaemic hemispheres of Ctsk$^{+/+}$/MCAO/rtPA mice as compared to that of sham-surgery mice, indicating disruption of the BBB. Significantly more extravasated EB dye was seen in Ctsk$^{-/-}$/MCAO/rtPA mice than in Ctsk$^{+/+}$/MCAO/rtPA mice (Fig. 3b), indicating that Ctsk deficiency aggravates BBB disruption after cerebral ischaemia.

Western blot analysis of ischaemic brain conducted 24 h after MCAO indicates that expression of the tight junction proteins occludin and claudin-5, essential for maintaining BBB integrity, was suppressed in Ctsk$^{+/+}$/MCAO/rtPA mice as compared to sham-surgery mice. Ctsk$^{-/-}$/MCAO/rtPA mice expressed much less occludin and claudin-5 than did Ctsk$^{+/+}$/MCAO/rtPA mice (Fig. 3c).

## Ctsk Knockout Induces VEGF Expression in MCAO/rtPA-Induced HT Mice and the Expression of Akt/mTOR Pathway

Because increased VEGF expression is associated with BBB leakage in the acute ischaemic brain, we examined VEGF expression in rtPA-induced HT after MCAO. Western blot analysis revealed that cerebral ischaemia significantly increased VEGF expression over that of sham-surgery mice and that VEGF expression was higher in Ctsk$^{-/-}$/MCAO/rtPA mice than in Ctsk$^{+/+}$/MCAO/rtPA mice (Fig. 4a). Double immunostaining revealed that VEGF primarily colocalised with CD31-positive blood vessels at 24 h after stroke. Consistent with the western blot results, VEGF immunoreactivity in CD31-positive vascular endothelium in the peri-infarct area was elevated in Ctsk$^{-/-}$/MCAO/rtPA mice as compared to Ctsk$^{+/+}$/MCAO/rtPA mice (Fig. 4b).

To test the expression of Akt-TOR pathway, we compared the expression of Akt, p-Akt, mTOR and p-mTOR between the different mice. Western blot analysis showed that cerebral ischaemia reduced Akt phosphorylation (p-Akt/Akt) and mTOR phosphorylation (p-mTOR/mTOR). This effect was significantly greater in Ctsk$^{-/-}$/MCAO/rtPA mice than in Ctsk$^{+/+}$/MCAO/rtPA mice (Fig. 4c, d).

## Discussion

rtPA, the only approved drug for the treatment of AIS, has provided excellent outcomes for many patients but imposes an increased risk of HT, a life-threatening complication. Here we observed greater HT, cerebral oedema, BBB disruption, neurological deficits and infarct volume in Ctsk knockout mice than in wild-type mice. These results suggest that Ctsk protects against rtPA-induced HT after cerebral ischaemia.

Although the precise mechanism whereby rtPA induces HT after ischaemia remains elusive, experimental and clinical evidence indicates that neurovascular unit disruption is likely a major contributor (Fagan et al. 2004; Wang and Lo 2003). The BBB is a vital component of the neurovascular

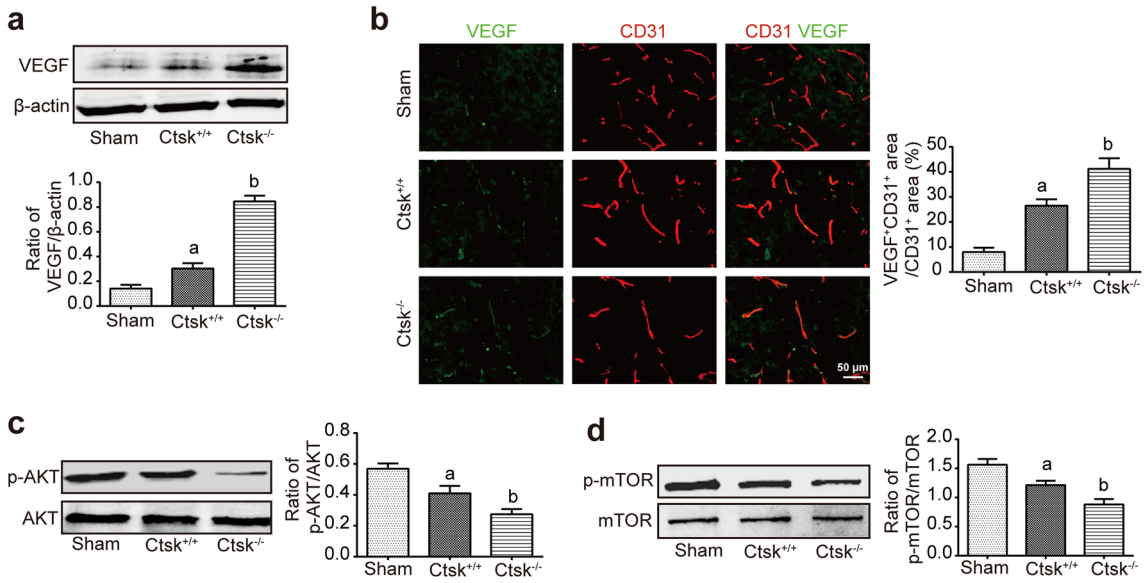


**Fig. 4** Elevated VEGF expression in Ctsk$^{-/-}$/MCAO/rtPA mice via Akt/mTOR pathway activation. **a** Western blot analysis of VEGF expression in ischaemic hemisphere lysates from mice of different groups. VEGF expression was greater in Ctsk$^{+/+}$/MCAO/rtPA (Ctsk$^{+/+}$) mice than in sham-surgery mice, with the expression level greater in Ctsk$^{-/-}$/MCAO/rtPA (Ctsk$^{-/-}$) than in Ctsk$^{+/+}$/MCAO/rtPA mice. **b** Double immunostaining of mouse brain coronal sections with anti-VEGF (green) and anti-CD31 (red). The number of VEGF immunoreactive cells in vascular endothelium was determined by counting VEGF+/CD31+ cells in brain sections. The number of VEGF+/CD31+ cells was higher in Ctsk$^{+/+}$/MCAO/rtPA than in sham-surgery mice, with more VEGF+/CD31+cells in Ctsk$^{-/-}$/MCAO/rtPA than in Ctsk$^{+/+}$+MCAO+rtPA mice. **c**, **d** Western blot of Akt, p-Akt, mTOR and p-mTOR in ischaemic hemisphere lysates from mice of different groups. p-Akt/Akt and p-mTOR/mTOR ratios were higher in Ctsk$^{+/+}$/MCAO/rtPA than in sham-surgery mice, and lower in Ctsk$^{-/-}$/MCAO/rtPA than in Ctsk$^{+/+}$/MCAO/rtPA mice. $^{a}p<0.05$, sham versus Ctsk$^{+/+}$; $^{b}p<0.05$, Ctsk$^{-/-}$ versus Ctsk$^{+/+}$

unit, containing tight junctional (TJ) proteins and transporters of ions and nutrients that maintain normal brain physiology. Ischaemic stroke-induced BBB breakdown promotes complications such as cerebral oedema and HT, especially in association with therapeutic recanalisation of occluded vessels (Horsch et al. 2015; Kono et al. 2014). Further rupture of the BBB damages the entire neurovascular unit, including the extracellular matrix, endothelial cells, astrocytes, neurons and pericytes. The involvement of Ctsk in protecting against this process is supported by our observation that Ctsk knockout mice exhibited more brain oedema, greater BBB disruption and greater numbers of apoptotic neurons and IBA-1 positive cell than did Ctsk$^{+/+}$/MCAO/rtPA mice. Thus, Ctsk deficiency might cause greater HT by altering the neurovascular unit and disrupting the BBB. Our findings are consistent with those of Jiang et al., who report that functional recovery after femoral artery ligation-induced ischaemia is impaired in Ctsk-deficient mice (Jiang et al. 2014). These authors observed that in response to hypoxia, Ctsk activates Notch-1, leading to downstream activation of the Akt/mTOR/VEGF pathway. Thus, the absence of such signalling is implicated in the greater degree of HT observed in Ctsk-deficient mice.

As a potent mediator of endothelial proliferation and migration, VEGF is associated with angiogenesis, neurogenesis, axon plasticity, neuron survival and vascular permeability. VEGF also plays an important role in the development of brain oedema during ischaemic stroke (Greenberg and Jin 2013; Zhang et al. 2017b). VEGF expression is upregulated in peri-infarct regions within 3 h of the onset of ischaemia (Hayashi et al. 1997). Early administration of VEGF to ischaemic rat brains is reported to increase BBB leakage, induce HT, increase the infarct size in the brain (Zhang et al. 2000), as well as induce the apoptotic death of neurons. In rats, inhibition of the VEGF signalling pathway was observed to attenuate HT after rtPA treatment (Kanazawa et al. 2011). In the absence of Ctsk, we observed elevated levels of VEGF after rtPA treatment of MCAO mice. Thus, we propose that Ctsk may protect against HT by inhibiting VEGF expression.

VEGF expression is regulated by the Akt/mTOR signalling pathway (Park et al. 2016; Sarnelli et al. 2016; Zeng et al. 2017; Zhang et al. 2017a). Studies suggest that the degree and duration of mTOR signalling may be an essential factor in neuroprotection (Maiese et al. 2013). mTOR activation can foster long-term potentiation and synaptic plasticity in models of Alzheimer's disease (Ma et al. 2010) and block inflammatory cell death during toxic β-amyloid exposure (Shang et al. 2012). However, sustained activation of mTOR can result in impaired neuronal

stem cell maturation (Uzdensky et al. 2013) and clinical disability with dyskinesia in Parkinson's disease patients (Chong et al. 2011). Prolonged inhibition of mTOR can lead to neuron death (Jessen et al. 2010). Consistent with these findings, we observed that Ctsk knockout results in significantly higher VEGF expression and significantly lower levels of phospo-Akt and phospo-mTOR compared to wild-type mice. These findings suggest that suppression of Akt/mTOR signalling due to the absence of Ctsk induces apoptotic cell death in the peri-infarct area of $Ctsk^{-/-}$/MCAO/rtPA mice, disrupting BBB integrity and altering its permeability. In response, VEGF expression increases, leading to apoptotic cell death via VEGF/VEGFR2 signalling.

This study has several limitations. The extent and mechanism underlying the protective effect of Ctsk is unclear and requires further study. Determining the mechanism whereby Ctsk affects Akt-mTOR-VEGF signalling will require studies using pathway inhibitors. The relevance of these findings to clinical applications must be determined by examining the expression of Ctsk in AIS patients and investigating the relationship between Ctsk expression level and the occurrence of rtPA-induced HT.

In conclusion, Ctsk knockout resulted in damage to the neurovascular unit and induced BBB breakdown, likely by affecting the Akt-mTOR-VEGF signalling cascade. These results suggest that Ctsk administration has the potential as a novel modality for improving the safety of rtPA following stroke.

**Author Contributions** RZ, XWH, YHS and YSL performed the major experiments and wrote the draft manuscript. FDL, YH, MTZ, XYF, LZ, BQZ and HQL performed the experiments and acquired the data, participated in drafting of the manuscript, created the figures and revised the manuscript. GPS and JRL designed the study and revised the manuscript for important intellectual content. All authors read and approved the final manuscript.

**Funding** This study was funded by the National Natural Science Foundation of China (No. 81271302 to J.R. Liu and 81500907 to L. Zhao), research innovation project from Shanghai municipal science and technology commission (No. 14JC1404300, to J.R. Liu), the "prevention and control of chronic diseases project" of Shanghai Hospital Development Center (No. SHDC12015310, to J.R. Liu), Project from SHSMU-ION Research Center for Brain Disorders (No. 2015NKX006, to J.R. Liu), project from Shanghai Municipal Education Commission—Gaofeng Clinical Medicine Grant Support (No. 20161422 to J.R. Liu), Clinical Research Project from Shanghai Jiao Tong University School of Medicine (No. DLY201614 to J.R. Liu) and Biomedicine Key program from Shanghai Municipal Science and Technology Commission (No. 16411953100 to J.R. Liu).

## Compliance with Ethical Standards

**Conflict of interest** The authors declare that they have no conflict of interest.

**Ethical Approval** All applicable international, national and/or institutional guidelines for the care and use of animals were followed.

## References

Aoki T, Kataoka H, Ishibashi R, Nozaki K, Hashimoto N (2008) Cathepsin B, K, and S are expressed in cerebral aneurysms and promote the progression of cerebral aneurysms. Stroke 39:2603–2610. https://doi.org/10.1161/STROKEAHA.107.513648

Bernstein HG, Bukowska A, Dobrowolny H, Bogerts B, Lendeckel U (2007) Cathepsin K and schizophrenia. Synapse 61:252–253. https://doi.org/10.1002/syn.20358

Bohley P, Seglen PO (1992) Proteases and proteolysis in the lysosome. Experientia 48:151–157

Chong ZZ, Hou J, Shang YC, Wang S, Maiese K (2011) EPO relies upon novel signaling of Wnt1 that requires Akt1, FoxO3a, GSK-3beta, and beta-catenin to foster vascular integrity during experimental diabetes. Curr Neurovasc Res 8:103–120

Dauth S et al (2011) Cathepsin K deficiency in mice induces structural and metabolic changes in the central nervous system that are associated with learning and memory deficits. BMC Neurosci 12:74. https://doi.org/10.1186/1471-2202-12-74

Dauth S, Schmidt MM, Rehders M, Dietz F, Kelm S, Dringen R, Brix K (2012) Characterisation and metabolism of astroglia-rich primary cultures from cathepsin K-deficient mice. Biol Chem 393:959–970. https://doi.org/10.1515/hsz-2012-0145

Fagan SC, Hess DC, Hohnadel EJ, Pollock DM, Ergul A (2004) Targets for vascular protection after acute ischemic stroke. Stroke 35:2220–2225. https://doi.org/10.1161/01.STR.0000138023.60272.9e

Fukuda S, Fini CA, Mabuchi T, Koziol JA, Eggleston LL Jr, del Zoppo GJ (2004) Focal cerebral ischemia induces active proteases that degrade microvascular matrix. Stroke 35:998–1004. https://doi.org/10.1161/01.STR.0000119383.76447.05

Greenberg DA, Jin K (2013) Vascular endothelial growth factors (VEGFs) and stroke. Cell Mol Life Sci 70:1753–1761. https://doi.org/10.1007/s00018-013-1282-8

Hayashi T, Abe K, Suzuki H, Itoyama Y (1997) Rapid induction of vascular endothelial growth factor gene expression after transient middle cerebral artery occlusion in rats. Stroke 28:2039–2044

Hong JM, Lee JS, Song HJ, Jeong HS, Choi HA, Lee K (2014) Therapeutic hypothermia after recanalization in patients with acute ischemic stroke. Stroke 45:134–140. https://doi.org/10.1161/STROKEAHA.113.003143

Horsch AD et al (2015) Relation between reperfusion and hemorrhagic transformation in acute ischemic stroke. Neuroradiology 57:1219–1225. https://doi.org/10.1007/s00234-015-1577-6

Jessen N et al (2010) Ablation of LKB1 in the heart leads to energy deprivation and impaired cardiac function. Biochim Biophys Acta 1802:593–600. https://doi.org/10.1016/j.bbadis.2010.04.008

Jiang H et al (2014) Cathepsin K-mediated Notch1 activation contributes to neovascularization in response to hypoxia. Nat Commun 5:3838. https://doi.org/10.1038/ncomms4838

Jickling GC, Liu D, Stamova B, Ander BP, Zhan X, Lu A, Sharp FR (2014) Hemorrhagic transformation after ischemic stroke in animals and humans. J Cereb Blood Flow Metab 34:185–199. https://doi.org/10.1038/jcbfm.2013.203

Kanazawa M et al (2011) Inhibition of VEGF signaling pathway attenuates hemorrhage after tPA treatment. J Cereb Blood Flow Metab 31:1461–1474. https://doi.org/10.1038/jcbfm.2011.9

Khurana D, Das B, Kumar A, Kumar SA, Khandelwal N, Lal V, Prabhakar S (2017) Temporal trends in intravenous thrombolysis in acute ischemic stroke: experience from a tertiary care center

in India. J Stroke Cerebrovasc Dis 26:1266–1273. https://doi.org/10.1016/j.jstrokecerebrovasdis.2017.01.019
Kono S et al (2014) Rivaroxaban and apixaban reduce hemorrhagic transformation after thrombolysis by protection of neurovascular unit in rat. Stroke 45:2404–2410. https://doi.org/10.1161/STROKEAHA.114.005316
Lansberg MG, Albers GW, Wijman CA (2007) Symptomatic intracerebral hemorrhage following thrombolytic therapy for acute ischemic stroke: a review of the risk factors. Cerebrovasc Dis 24:1–10. https://doi.org/10.1159/000103110
Ma T et al (2010) Dysregulation of the mTOR pathway mediates impairment of synaptic plasticity in a mouse model of Alzheimer's disease. PLoS One 5:55. https://doi.org/10.1371/journal.pone.0012845
Maiese K, Chong ZZ, Shang YC, Wang S (2013) mTOR: on target for novel therapeutic strategies in the nervous system. Trends Mol Med 19:51–60. https://doi.org/10.1016/j.molmed.2012.11.001
Morris DC (2008) Thrombolysis 3 to 4.5 hours after acute ischemic stroke. N Engl J Med 359:2841 **author reply 2841**
Nour M, Scalzo F, Liebeskind DS (2013) Ischemia-reperfusion injury in stroke. Interv Neurol 1:185–199. https://doi.org/10.1159/000353125
Novinec M, Grass RN, Stark WJ, Turk V, Baici A, Lenarcic B (2007) Interaction between human cathepsins K, L, and S and elastins: mechanism of elastinolysis and inhibition by macromolecular inhibitors. J Biol Chem 282:7893–7902. https://doi.org/10.1074/jbc.M610107200
Park JH, Yoon J, Park B (2016) Pomolic acid suppresses HIF1alpha/VEGF-mediated angiogenesis by targeting signaling cascades. Phytomedicine 23:1716–1726. https://doi.org/10.1016/j.phymed.2016.10.010
Pena ID, Borlongan C, Shen G, Davis W (2017) Strategies to extend thrombolytic time window for ischemic stroke treatment: an unmet clinical need. J Stroke 19:50–60. https://doi.org/10.5853/jos.2016.01515
Platt MO, Shockey WA (2016) Endothelial cells and cathepsins: biochemical and biomechanical regulation. Biochimie 122:314–323. https://doi.org/10.1016/j.biochi.2015.10.010
Saftig P, Hunziker E, Wehmeyer O, Jones S, Boyde A, Rommerskirch W, Moritz JD, Schu P, von Figura K (1998) Impaired osteoclastic bone resorption leads to osteopetrosis in cathepsin-K-deficient mice. Proc Natl Acad Sci USA 95(23):13453–13458
Sarnelli G et al (2016) Palmitoylethanolamide modulates inflammation-associated vascular endothelial growth factor (VEGF) signaling via the Akt/mTOR pathway in a selective peroxisome proliferator-activated receptor alpha (PPAR-alpha)-dependent manner. PLoS ONE 11:56198. https://doi.org/10.1371/journal.pone.0156198
Shahjouei S, Cai PY, Ansari S, Sharififar S, Azari H, Ganji S, Zand R (2016) Middle cerebral artery occlusion model of stroke in rodents: a step-by-step approach. J Vasc Interv Neurol 8:1–8
Shang YC, Chong ZZ, Wang S, Maiese K (2012) Prevention of beta-amyloid degeneration of microglia by erythropoietin depends on Wnt1, the PI 3-K/mTOR pathway, Bad, and Bcl-xL. Aging 4:187–201. https://doi.org/10.18632/aging.100440
Sumii T, Lo EH (2002) Involvement of matrix metalloproteinase in thrombolysis-associated hemorrhagic transformation after embolic focal ischemia in rats. Stroke 33:831–836
Uzdensky AB, Demyanenko SV, Bibov MY (2013) Signal transduction in human cutaneous melanoma and target drugs. Curr Cancer Drug Targets 13:843–866
Wang X, Lo EH (2003) Triggers and mediators of hemorrhagic transformation in cerebral ischemia. Mol Neurobiol 28:229–244. https://doi.org/10.1385/MN:28:3:229
Wang L et al (2013) Recombinant ADAMTS13 reduces tissue plasminogen activator-induced hemorrhage after stroke in mice. Ann Neurol 73:189–198. https://doi.org/10.1002/ana.23762
Wang W, Li M, Chen Q, Wang J (2015) Hemorrhagic transformation after tissue plasminogen activator reperfusion therapy for ischemic stroke: mechanisms, models, and biomarkers. Mol Neurobiol 52:1572–1579. https://doi.org/10.1007/s12035-014-8952-x
Wardlaw JM, Koumellis P, Liu M (2013) Thrombolysis (different doses, routes of administration and agents) for acute ischaemic stroke. Cochrane Database Syst Rev. https://doi.org/10.1002/14651858.cd000514.pub3
Zeng B, Liu L, Wang S, Dai Z (2017) ILK regulates MSCs survival and angiogenesis partially through AKT and mTOR signaling pathways. Acta Histochem 119:400–406. https://doi.org/10.1016/j.acthis.2017.04.003
Zhang ZG et al (2000) VEGF enhances angiogenesis and promotes blood-brain barrier leakage in the ischemic brain. J Clin Invest 106:829–838. https://doi.org/10.1172/JCI9369
Zhang F, Chen X, Wei K, Liu D, Xu X, Zhang X, Shi H (2017a) Identification of key transcription factors associated with lung squamous cell carcinoma. Med Sci Monit 23:172–206
Zhang HT et al (2017b) Early VEGF inhibition attenuates blood-brain barrier disruption in ischemic rat brains by regulating the expression of MMPs. Mol Med Rep 15:57–64. https://doi.org/10.3892/mmr.2016.5974